FANCJ couples replication past natural fork barriers with maintenance of chromatin structure

Rebekka A. Schwab,[1] Jadwiga Nieminuszczy,[1,2] Kazuo Shin-ya,[3] and Wojciech Niedzwiedz[1]

[1]The Weatherall Institute of Molecular Medicine, Oxford University, Oxford OX3 9DS, England, UK
[2]Institute of Biochemistry and Biophysics, PAS, 02-106 Warsaw, Poland
[3]Biomedicinal Information Research Center, National Institute of Advanced Industrial Science and Technology, Koto-ku, Tokyo 135-0064, Japan

Defective DNA repair causes Fanconi anemia (FA), a rare childhood cancer–predisposing syndrome. At least 15 genes are known to be mutated in FA; however, their role in DNA repair remains unclear. Here, we show that the FANCJ helicase promotes DNA replication in trans by counteracting fork stalling on replication barriers, such as G4 quadruplex structures. Accordingly, stabilization of G4 quadruplexes in ΔFANCJ cells restricts fork movements, uncouples leading- and lagging-strand synthesis and generates small single-stranded DNA gaps behind the fork. Unexpectedly, we also discovered that FANCJ suppresses heterochromatin spreading by coupling fork movement through replication barriers with maintenance of chromatin structure. We propose that FANCJ plays an essential role in counteracting chromatin compaction associated with unscheduled replication fork stalling and restart, and suppresses tumorigenesis, at least partially, in this replication-specific manner.

Introduction

Homozygous mutations in FANCJ cause Fanconi anemia (FA), a cancer-predisposing disorder characterized by high genomic instability and hypersensitivity to DNA interstrand cross-link (ICL)–inducing agents. Monoallelic mutations in FANCJ are associated with two- to threefold increased breast cancer susceptibility, suggesting an essential function in tumor suppression (Hiom, 2010). This is further supported by the direct interaction of FANCJ with the hereditary breast cancer–associated gene product BRCA1 (Cantor et al., 2001). In contrast to most other FA proteins that do not contain obvious enzymatic domains, FANCJ contains a highly conserved N-terminal helicase domain of the superfamily (II) subtype. In line with this, biochemical characterization of the purified protein showed 5′–3′ helicase activity in vitro, with preference for duplex DNA containing either a short 3′ or 5′ single-stranded region. FANCJ also binds and unwinds branched DNA structures, 5′ flaps, and D-loops, suggesting its possible involvement in the processing of replication intermediates (Gupta et al., 2005). Several lines of evidence indicate a central role for its helicase activity in the maintenance of genome stability. First, all FANCJ mutations genetically linked to FA are clustered within the helicase core domain, and patient-derived mutant forms of FANCJ exhibit impaired helicase activity (Hiom, 2010). Second, FANCJ mutants and/or cells complemented with plasmids expressing the helicase-dead protein are hypersensitive to replication inhibitors such as cisplatin or hydroxyurea (HU; Hiom, 2010; Suhasini et al., 2011).

Eukaryotic genomic DNA is packed into a highly condensed chromatin structure where the repeating nucleosomes form the basic unit. Chromatin can be roughly divided into heterochromatin (silenced) or euchromatin (active) states that are defined by their degree of compaction as well as their occupancy by specific combinations of modified histones, which are involved in regulating chromatin formation. During DNA replication, chromatin has to be dismantled ahead of the progressing replicative fork, and then faithfully reassembled in heterochromatic or euchromatic form behind the fork in order to preserve genomic and epigenetic information. How discrete chromatin domains are accurately inherited during DNA replication is still poorly understood. Moreover, there is increasing evidence that replicative stress affects faithful chromatin restoration (Jasencakova et al., 2010; Sarkies et al., 2010). Recently, unusual DNA structures, such as G quartets, have been suggested as a potent source of genomic instability due to their ability to disrupt

R.A. Schwab and J. Nieminuszczy contributed equally to this paper.

Correspondence to Wojciech Niedzwiedz: wojciech.niedzwiedz@imm.ox.ac.uk

Abbreviations used in this paper: CldU, chlorodeoxyuridine; FA, Fanconi anaemia; HU, hydroxyurea; IdU, iododeoxyuridine; MNase, micrococcal nuclease; ssDNA, single-stranded DNA; WT, wild type.

The Rockefeller University Press $30.00
J. Cell Biol. Vol. 201 No. 1 33–48
www.jcb.org/cgi/doi/10.1083/jcb.201208009

the normal progression of replication forks (Branzei and Foiani, 2010; Paeschke et al., 2011). Interestingly, the unwinding of such atypical, guanine-rich DNA structures, termed G4 quadruplex DNA motifs, was recently identified as a novel function of FANCJ (Wu et al., 2008). In support of its role in this process, patient-derived FANCJ cells, as well as *Caenorhabditis elegans* FANCJ mutants (dog-1), exhibit genomic deletions in the vicinity of DNA sequences containing the G4 signature (Cheung et al., 2002; London et al., 2008). Likewise, transcriptional profiling of chicken DT40 cells lacking FANCJ suggests a possible role for the protein in coordination of two pathways required to maintain epigenetic stability near G4 DNA motifs (Sarkies et al., 2012). However, we still have a limited mechanistic understanding of how FANCJ facilitates replication to promote genomic and epigenetic integrity, and suppresses tumorigenesis.

Here we show that, despite its broad sensitivity to replication inhibitors, FANCJ is dispensable for replisome stability. Instead, it promotes efficient replication fork movement in trans by counteracting fork stalling on replication fork barriers. Surprisingly, we also discovered that alterations to replication fork movement increase chromatin compaction in the DT40 FANCJ mutant, resulting in reorganization of chromatin structure. We propose that FANCJ plays a crucial role in the maintenance of genomic and epigenetic integrity by facilitating fork movement past natural DNA structure–mediated replication barriers. This function requires its helicase activity and is independent of the functional FA pathway.

Results

FANCJ helicase activity prevents fork stalling and inhibition of DNA synthesis under conditions of replicative stress

To investigate the role of FANCJ in DNA replication we first analyzed survival of a pair of isogenic DT40 cell lines, wild type (WT) or FANCJ null, exposed to agents that impede this process. In line with its putative role in DNA replication we observed that FANCJ-null mutants are hypersensitive not only to HU as reported recently (Suhasini and Brosh, 2012), but also to other anticancer drugs that interfere with DNA synthesis, such as camptothecin and aphidicolin (Fig. 1 A).

To gain a more detailed insight into the role of FANCJ during DNA replication, we analyzed DNA synthesis in these isogenic cells using the DNA fiber technique as described previously (Schwab et al., 2010). Unperturbed WT and ΔFANCJ cells showed similar replication fork velocity, with an average fork progression rate of around 1 kb/min (Fig. S1, A–C). Given that FANCJ is recruited to blocked replication forks (Zhang et al., 2010) and FANCJ-deficient cells were hypersensitive to replication inhibitors (Fig. 1 A), we next investigated the effect of perturbing DNA synthesis with a low dose of HU for up to 60 min. This treatment should result in replication fork stalling rather than collapse (Petermann et al., 2010). A schematic diagram showing the experimental design as well as representative images of individual DNA fibers are presented in Fig. 1 B. Transient exposure of ΔFANCJ cells to HU (20–60 min) caused a statistically significant reduction (30%; $P < 0.0001$) in average fork velocity in comparison to WT (Fig. 1 C). Furthermore, the fork ratio (chlorodeoxyuridine [CldU] tract length/iododeoxyuridine [IdU] tract length) distribution curves of ΔFANCJ cells show a greater leftward shift compared with the curve derived from WT cells, indicating fork slowing (Fig. 1 D). A similar effect was also observed with a higher dose of HU (Fig. S2).

Next we analyzed whether the enzymatic function of FANCJ was required to promote efficient DNA synthesis upon replicative stress. To test this, we generated two independent clones of ΔFANCJ complemented with cDNA coding for either the WT human FANCJ protein or its helicase-inactive FANCJ-K52R form as described previously (Bridge et al., 2005) (Fig. 2 A). Cell survival analyses showed that expression of the WT protein, but not the helicase-dead variant, reverses the hypersensitivity to HU (Fig. 2 B). Analysis of fork velocity in the complemented lines showed that the WT protein was capable of restoring normal dynamics of replication forks in response to HU treatment (Fig. 2, C and D; $P < 0.0001$). In contrast, helicase-dead mutants displayed impaired replication dynamics (Fig. 2, C and D; $P < 0.0001$).

To identify the molecular mechanism responsible for decreased fork velocity in ΔFANCJ cells, we monitored the fates of two sister forks traveling in opposite directions from the same origin of replication (Blackford et al., 2012). Because forks from the same origin tend to display similar replication rates, we reasoned that an overall decrease in the rate of DNA polymerization would affect both sister forks (Conti et al., 2007). Conversely, if individual forks are more prone to stalling, this would cause greater asymmetry between sister fork tract lengths. These two possibilities are shown schematically in Fig. 3 A. We noticed a significant ($P < 0.006$) increase in asymmetric sister forks in ΔFANCJ cells (Fig. 3 B). Again, introducing wild-type FANCJ but not the helicase-dead (FANCJ-K52R) mutant reversed the fork asymmetry phenotype (Fig. 3 C; $P < 0.004$). This indicates that fork stalling occurs at a higher rate in cells lacking FANCJ or its helicase activity, possibly reflecting an inability to efficiently replicate through hard-to-replicate DNA sequences.

FANCJ is dispensable for replication fork stability

Having established that FANCJ's enzymatic activity plays a key role in limiting the accumulation of stalled forks upon exposure to low doses of HU, we next examined the stability of these forks. To assess fork integrity, we measured the kinetics of double-strand break (DSB) formation in HU-treated WT and ΔFANCJ cells by neutral comet assay. In both cell lines, HU treatment induced DSBs ($P < 0.0001$); however, we were unable to detect any significant excess of DSB formation in FANCJ mutant cells compared with WT DT40 (Fig. 3 D). Given the above, we hypothesized that stalled replisomes remain replication proficient and are capable of restarting DNA synthesis upon removal of the blockade. To test this, we modified our fiber protocol to allow for analysis of fork restart as described previously (Fig. 3 E; Schwab et al., 2010; Blackford et al., 2012). We noticed an initial delay in restarting stalled forks in ΔFANCJ cells; however, 20 min after HU removal both cell lines showed a similar number of active forks (Fig. 3 F). Moreover, the newly

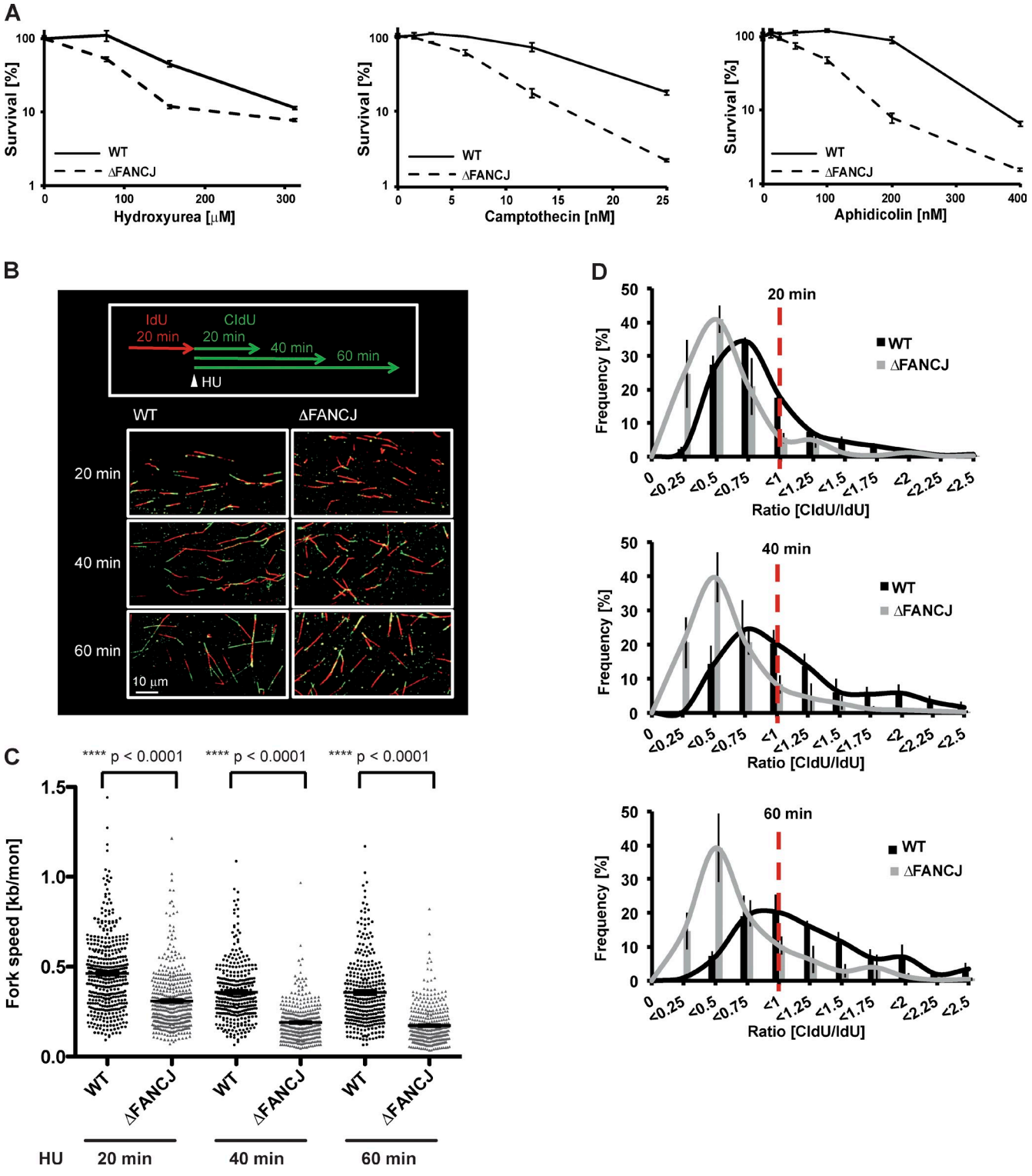

Figure 1. **FANCJ suppresses hypersensitivity to replication inhibitors and stabilizes elongating forks when DNA replication is impaired.** (A) Sensitivity assays for WT and ΔFANCJ DT40 cells in response to hydroxyurea, camptothecin, and aphidicolin as measured by MTS survival assay. Mean values of representative experiments performed in triplicate are shown ± SD. (B) The cartoon depicts a schematic of the fiber-labeling and HU treatment procedure. Representative fiber pictures from WT and ΔFANCJ cells treated with 0.2 mM HU for different times during the CldU pulse are shown on the bottom. (C) Dot plots of individual fork speeds of WT and ΔFANCJ cells in the presence of HU. The mean and SEM are indicated ($n \geq 300$). (D) Distribution plots of the CldU/IdU ratio for different incubation periods with HU. Error bars represent SEM of three independent experiments ($n \geq 300$). Dashed line marks the CldU/IdU ratio equaling 1.

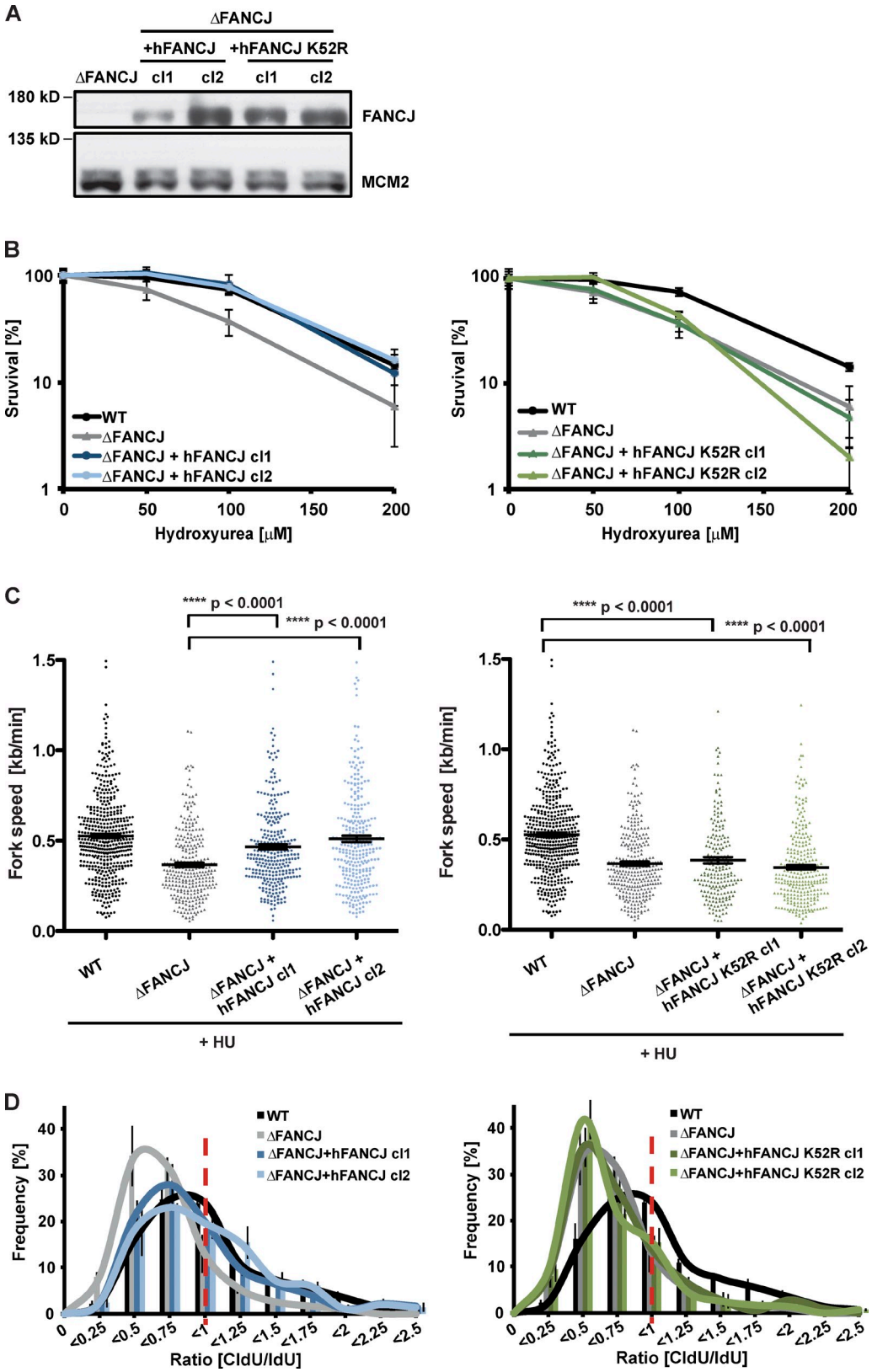

Figure 2. **The helicase domain of FANCJ is required for continuous replication fork elongation when replication is challenged.** (A) Western blot showing expression of FANCJ in two independent clones complemented with intact or helicase-dead FANCJ (FANCJ-K52R). (B) Cellular sensitivity of ΔFANCJ cells complemented with WT or FANCJ-K52R mutant clones to HU as measured by MTS survival assay. Error bars represent the SEM. (C) Dot plots represent individual replication fork velocities from HU-treated WT DT40 and ΔFANCJ complemented with WT or FANCJ-K52R cDNA including the mean ± SEM ($n \geq 300$). (D) Distribution plots of the CldU/IdU ratio of the FANCJ-complemented clones. Error bars represent the SEM of three independent experiments ($n \geq 300$).

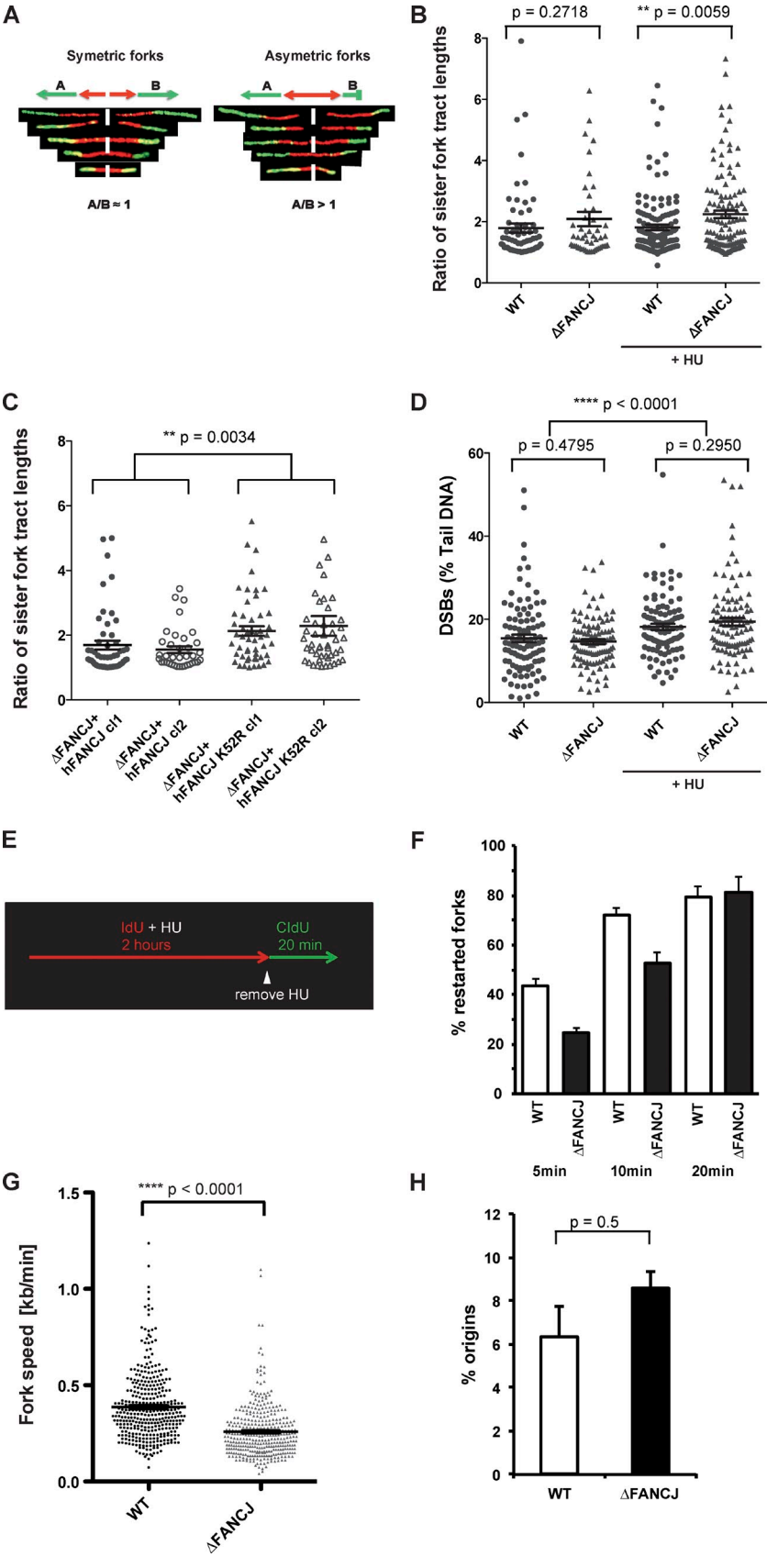

Figure 3. **Stalled replication forks in ΔFANCJ cells remain stable and retain the ability to restart DNA synthesis.** (A) Schematic showing examples of two normally progressing sister forks (symmetric) and a pair of sister forks with one fork stalled (asymmetric). (B) Dot plot of CldU tract length ratios of associated sister forks from untreated or HU-treated WT and ΔFANCJ cells ($n \geq 50$). (C) Dot plot of the ratio of two sister forks from ΔFANCJ cells complemented with WT or FANCJ-K52R cDNA with mean and SEM ($n \geq 50$). (D) The level of DNA double-strand breaks after HU exposure is measured by the neutral comet assay and represented as a percentage of tail DNA ($n = 90$). (E) Overview of the fiber-labeling procedure to measure recovery of DNA synthesis. (F) Recovery of DNA synthesis in response to 2 mM HU treatment in WT and ΔFANCJ cells ($n \geq 300$). (G) Replication tract lengths of the newly synthesized nascent strand upon fork restart after release from HU treatment ($n \geq 300$). (H) Analysis of newly fired origins in WT and ΔFANCJ cells treated with HU for 2 h. The graph represents the average of three independent experiments ± SEM ($n \geq 250$).

generated replication tracts in ΔFANCJ cells were significantly shorter than in the WT control (Fig. 3 G). This suggests that the initial delay in restarting DNA synthesis is most likely due to the time required to remove and/or bypass the blockade in the absence of FANCJ. Furthermore, both cell lines showed a similar level of new origin firing, suggesting that the restart of DNA synthesis is not driven by the firing of dormant origins within the vicinity of a stalled fork (Fig. 3 H). Taken together, these data suggest that during replication FANCJ promotes continuous DNA synthesis in trans by supporting fork passage through hard-to-replicate sites but is dispensable for maintaining replication fork stability. This view is further supported by previous studies in *C. elegans* and human cells showing that FANCJ is dispensable for the generation of a homologous recombination (HR) substrate at blocked forks as the mutant cells have normal kinetics of Rad51 focus formation in response to replication stress (Litman et al., 2005; Youds et al., 2008).

FANCJ is required to promote replication in the presence of the G4 stabilizer telomestatin

Exposure to HU adversely affects survival of *Pif1* mutant yeast cells by increasing fork stalling at G4 motifs (Paeschke et al., 2011). Significantly, FANCJ, like *Pif1*, unwinds G4 structures in vitro (London et al., 2008; Sanders, 2010). Therefore, we speculated that one possible explanation of the global increase in replication fork stalling we observed in ΔFANCJ cells could be impaired progression through natural DNA sequence-dependent replication fork barriers, such as G4 quadruplex motifs. To test this hypothesis we asked whether treatment with the highly specific G4-stabilizing ligand telomestatin (Lemarteleur et al., 2004) would impede replication fork movement. Surprisingly, we found that incubation of WT cells with a low dose of this agent for up to 24 h had little effect on replication speed (Fig. 4 A; $P = 0.5$). However, ΔFANCJ cells showed a significant decrease in replication fork velocity as well as an increased number of stalled (asymmetric) forks upon treatment with telomestatin (Fig. 4, A and B; $P < 0.0001$ and $P < 0.05$, respectively). Taken together, these results strongly suggest that FANCJ promotes efficient fork movement past DNA sequences that can form G4 quadruplexes.

FANCJ limits accumulation of single-stranded gaps behind the forks

Current models propose template switching or repriming downstream from the lesion as possible mechanisms used to allow the bypass of leading- or lagging-strand blockade, respectively (Branzei and Foiani, 2010). A block to lagging-strand synthesis could be relatively easy to overcome by a repriming event downstream of the impediment so that the fork would continue, leaving behind the blocking lesion in a single-stranded gap (Sogo et al., 2002; Fukui et al., 2004). Given the efficient fork restart observed in ΔFANCJ cells, we hypothesized that transient uncoupling of leading- and lagging-strand synthesis would allow "skipping" over the block in ΔFANCJ cells, leading to an efficient fork restart and generation of single-stranded DNA (ssDNA) gaps within the DNA template. To test this hypothesis directly we used the previously described gap-filling assay (Fukui et al., 2004; Fig. 4 C). This approach utilizes the DNA primer extension and translesion synthesis property of the T4 DNA polymerase. Importantly, because this polymerase does not have any strand displacement activity it can only fill in but not extend ssDNA gaps. We found a slight increase in the level of small unreplicated single-stranded gaps of 250–2000 bp in untreated ΔFANCJ cells as compared with the WT control, and this was further exacerbated in cells exposed to telomestatin for various times (Fig. 4 D). To solidify this observation we performed the same experiment, this time using increasing doses of telomestatin over a constant 24-h treatment period. Again we noticed a significant increase of labeled ssDNA gaps in ΔFANCJ cells (Fig. 4 E). Importantly, the size range of the labeled products (250–3000 bp) was similar to the nascent DNA products accumulating in the absence of Polδ, a polymerase required for lagging-strand primer extension (Fukui et al., 2004). Therefore, it is reasonable to assume that ssDNA gaps are generated between adjacent Okazaki fragments (Fukui et al., 2004). This supports our view that in the absence of FANCJ, stalled replication forks skip over DNA structure–dependent fork barriers on the lagging strand due to downstream repriming events. Because ssDNA has a higher propensity to form secondary structures, this is also consistent with the fact that unwinding of the parental duplex to allow multiple priming events within the looped-out lagging strand would lead to this strand becoming transiently single stranded. In line with this, electron microscopy (EM) of replication forks from untreated yeast cells showed the presence of short (200 bp) stretches of ssDNA (Sogo et al., 2002). This, at least theoretically, provides an opportunity for stable secondary structures, such as G-quadruplexes, to form on the lagging strand. Moreover, transient denaturation of the DNA duplex would also provide a binding space within the 5′ region of the looped-out DNA allowing for a helicase with 5′–3′ polarity, like FANCJ, to access and resolve structural barriers blocking the extension of a lagging-strand primer. In line with this, FANCJ is capable of efficiently binding and dissociating G4 quadruplexes with only 15 nucleotides of 5′-ssDNA tail (London et al., 2008). Because repriming downstream of the lesion on the leading strand would require reestablishment of the replication machinery outside of the origin, a process that has not been detected in vertebrates, we conclude that FANCJ promotes replication past structured fork barriers generated on the lagging strand. The unreplicated ssDNA gaps left behind the fork can be subsequently sealed by one of the post-replicative repair pathways.

FANCJ suppresses reorganization of chromatin structure

In the yeast model system, lagging-strand polymerase processivity is tightly coupled to nucleosome assembly behind the fork (Smith and Whitehouse, 2012). Given the significant increase in ssDNA gaps in ΔFANCJ cells, likely resulting from perturbation of the lagging-strand DNA synthesis, we tested whether this could lead to structural changes within the bulk mature chromatin. A classical approach to analyze chromatin structure relies on the use of certain nucleases such as micrococcal nuclease (MNase) and/or DNase I that can access and digest DNA within isolated cell nuclei (Bell et al., 2011). To examine the effect of

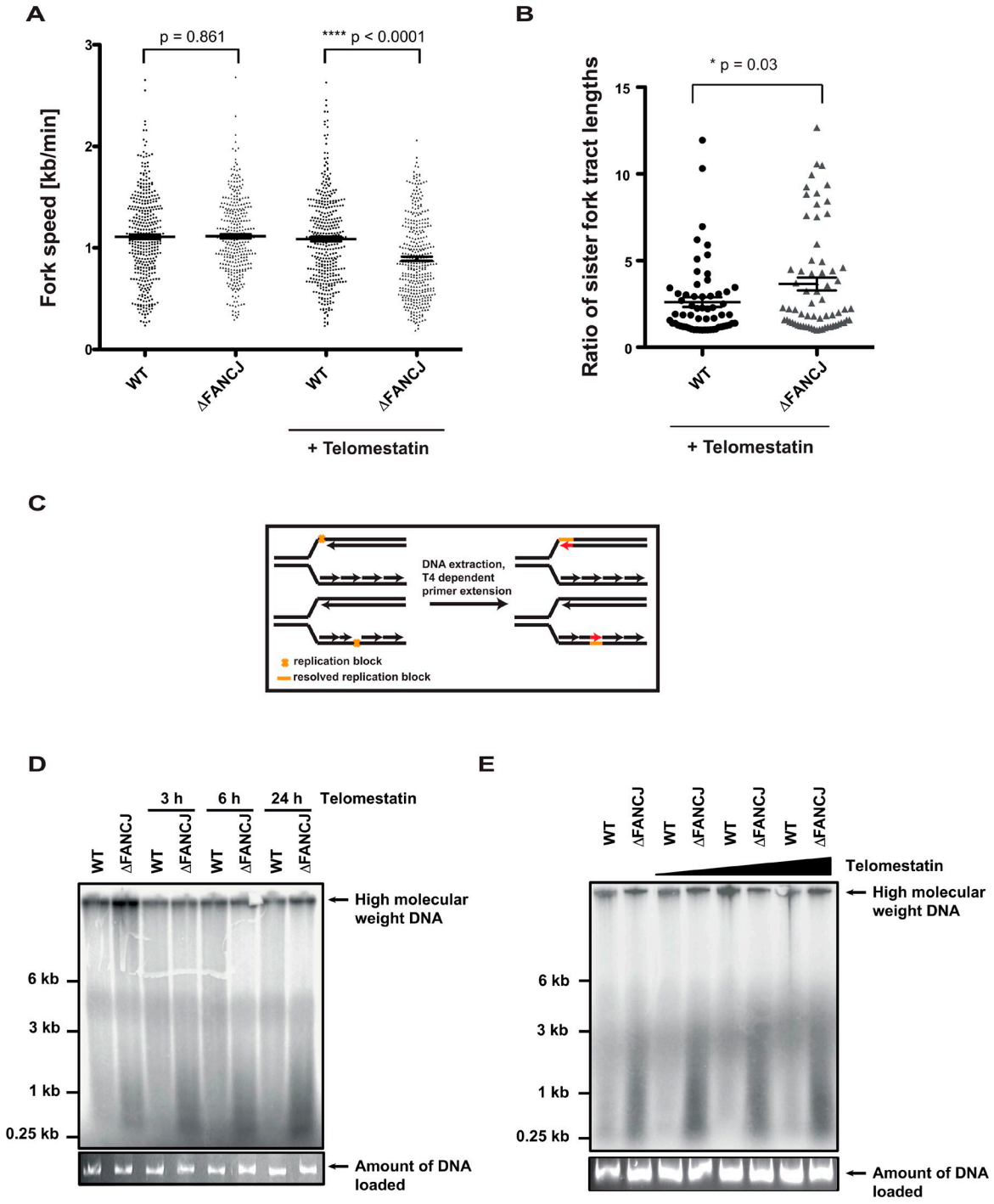

Figure 4. **ΔFANCJ cells accumulate ssDNA gaps due to their inability to replicate past DNA sequence–dependent fork barriers.** (A) Dot plot of fork speed of individual fibers from WT and ΔFANCJ cells either untreated or treated with 5 μM telomestatin for 24 h before subsequent labeling with IdU and CldU. Only continuously replicating red-green fibers were measured ($n \geq 300$). (B) Dot plot of CldU tract length ratios of associated sister forks from untreated or telomestatin-treated WT and ΔFANCJ cells ($n \geq 50$). (C) A schematic diagram of the gap-labeling procedure using T4 DNA polymerase. (D) DT40 cells were incubated with telomestatin for different times and genomic DNA was subsequently isolated and used as a template for the gap-filling assay using T4 DNA polymerase. ^{32}P-labeled DNA samples were resolved on an alkaline agarose gel, transferred onto a membrane, and scanned by a phosphorimager. Total genomic DNA run on a nondenaturing gel is shown below for quantification purposes. (E) WT and ΔFANCJ cells were treated with different doses of telomestatin for 24 h. The labeled nascent DNA extended by T4 polymerase was separated on a denaturing gel.

FANCJ disruption on the state of chromatin, we treated nuclei isolated from WT and ΔFANCJ cells with MNase. In WT cells chromatin was consistently and reproducibly more accessible to MNase digestion over various doses and time periods than in cells deficient in FANCJ (Fig. 5, A and B). This effect was already noticeable after a very short time, and to achieve a similar degree of chromatin digestion in both cell lines almost twice the time was required for FANCJ mutant cells (see Fig. 5, lanes 1 and

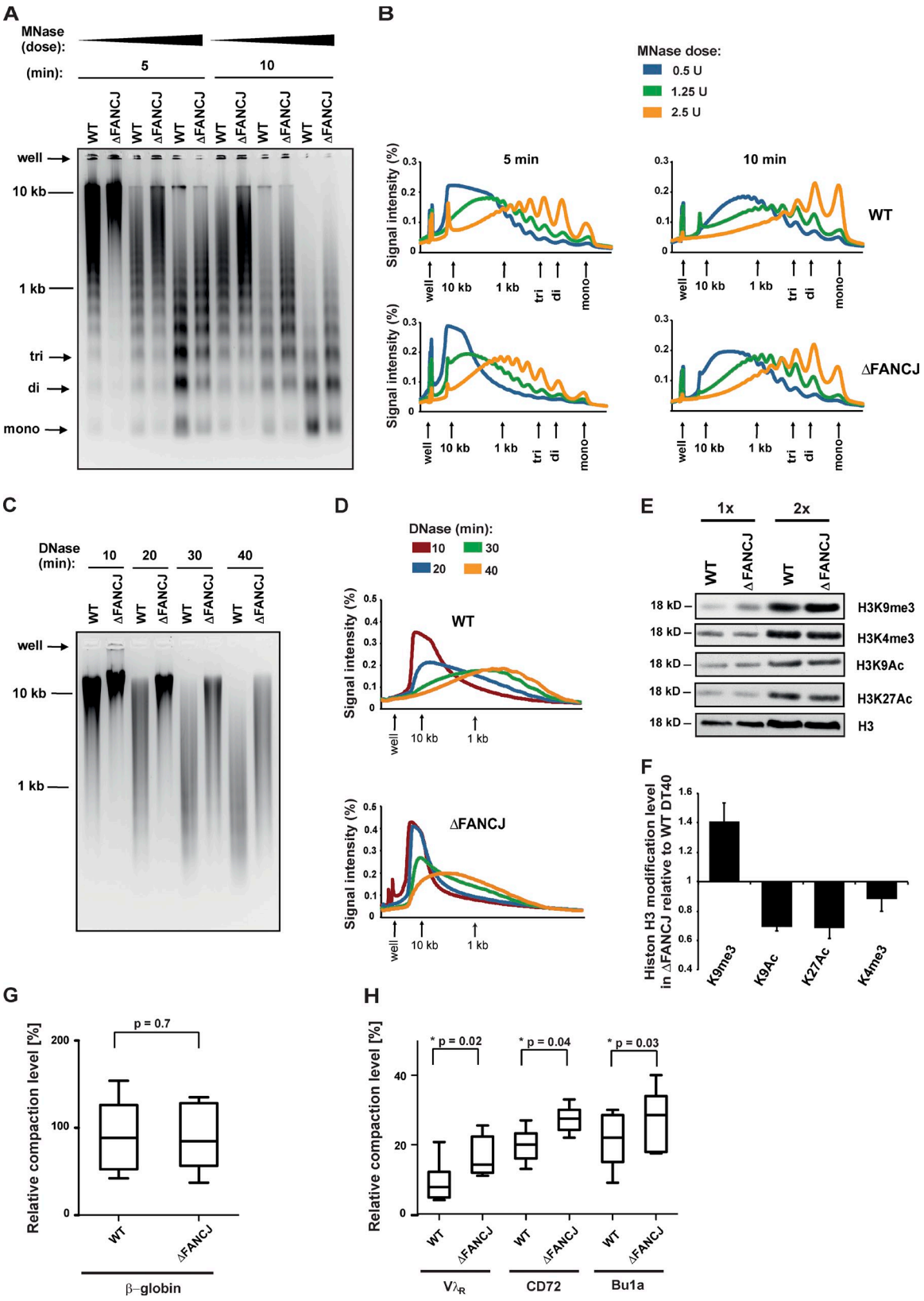

Figure 5. **Chromatin from ΔFANCJ cells displays reduced accessibility to nucleolytic digest.** (A) Nuclei from WT and ΔFANCJ cells were treated with 0.5, 1.25, or 2.5 U of MNase for the times indicated and DNA was analyzed on an agarose gel stained with ethidium bromide. (B) Quantification of the signal intensity of the gel shown in A. (C) DNase I digest of nuclei isolated from WT an ΔFANCJ cells and (D) signal intensity quantification of C. (E) Western blot of histone extracts from WT and ΔFANCJ cells probed with antibodies against the indicated histone modifications (1× and 2× extract loaded). (F) Quantification of histone marks in ΔFANCJ cells relative to WT ($n \geq 3$). (G and F) Semi-quantitative analysis of chromatin compaction within indicated genomic loci in ΔFANCJ and WT cells using EpiQ assay ($n \geq 4$).

8 or 3 and 10; and quantified signals). Next we performed a similar experiment but using DNase I to digest the isolated nuclei. Again we noticed a significant difference in chromatin accessibility across the entire time window tested (Fig. 5, C and D). To verify this observation we took advantage of the fact that histone posttranslational modifications are associated with the structural organization of chromatin. For example, trimethylation of histone H3 on lysine K9 provides a binding site for heterochromatin protein 1 (HP1) and is usually associated with a more closed chromatin structure. In contrast, acetylation of the same histone on lysine K9 or K27 and methylation on lysine K4 is associated with active chromatin (Bell et al., 2011). In support of the data presented above we found a significant increase in the histone mark associated with repressive chromatin (H3K9me3; $P < 0.05$), and a decrease in the histone marks associated with active chromatin (H3K9Ac and H3K27Ac; $P < 0.05$; Fig. 5, E and F).

To assess whether the observed change in chromatin compaction preferentially affects active (euchromatin) or already silenced domains (heterochromatin), we examined MNase digestion by Southern blot using probes against two well-characterized chromatin regions that harbor a G4 quadruplex forming motif; the constitutively heterochromatic β-globin locus (Litt et al., 2001) and an euchromatin locus coding for the Vλ immunoglobulin pseudogene array (Cummings et al., 2007). Probing within these domains showed an increase in chromatin compaction in ΔFANCJ cells as compared with WT. Interestingly, the euchromatin Vλ immunoglobulin locus appeared to be more affected (Fig. S3, A and B). Given the above, we analyzed two additional active loci, CD72 and Bu1a, which undergo silencing in ΔFANCJ cells (Sarkies et al., 2012). Again we noticed increased chromatin compaction within these loci in ΔFANCJ cells (Fig. S3, C and D). To verify this observation we used a semi-quantitative qPCR-based EpiQ chromatin analysis assay. This analysis confirmed an increase in chromatin compaction within the three active regions in ΔFANCJ cells in comparison to WT DT40, but not within the β-globin locus (Fig. 5, G and H; $P < 0.05$ and $P = 0.7$, respectively). These data suggest that in ΔFANCJ cells heterochromatin may form de novo within active domains. Surprisingly, restoring expression of FANCJ in ΔFANCJ cells corrected both the sensitivity and replication phenotype, but did not restore the wild-type chromatin structure (Fig. 6, A and B). Given the above, we considered the possibility that FANCJ disruption could affect adjacent genes, and/or the cell line acquired an additional mutation(s). This, however, seems unlikely, as we were unable to detect any significant change in the expression of genes located within 100 kb of the FANCJ locus (unpublished data); also, the analysis of two independently derived FANCJ-deficient clones showed similar changes in chromatin compaction as observed in our ΔFANCJ cell line (Fig. S3, E and F). Therefore, we conclude that altered replication fork movement in ΔFANCJ cells causes a significant increase in chromatin compaction, most likely affecting active regions of the genome.

Defective maturation of newly replicated chromatin in the FANCJ mutant

Given the above we wondered whether chromatin maturation could already be disrupted at the level of newly replicated DNA. To test this, we performed a similar experiment as described above, but this time after pulse-labeling the DNA with BrdU for 15 min. We reasoned that probing the DNA with an anti-BrdU antibody should allow us to specifically analyze changes in the structure of the newly replicated chromatin. We noticed an increased sensitivity to digestion of newly replicated DNA in WT cells as compared with the total DNA (Fig. 6, C–E; and Fig. S4, A–C), suggesting an incomplete maturation of the newly established chromatin at this time point. This is in agreement with previous data showing that newly replicated chromatin requires around 20 min to mature and to regain resistance to endonuclease cleavage (Seale, 1975). In contrast, BrdU-labeled DNA from ΔFANCJ cells showed higher resistance to both MNase and DNase I digestion (increased level of high molecular weight DNA corresponding to multiples of nucleosomes), suggesting a defect in faithful chromatin restoration on the newly replicated daughter strands (Fig. 6, C–E; and Fig. S4, A–C).

FANCJ suppresses reorganization of chromatin structure in a replication-dependent manner

To determine whether the helicase activity of FANCJ, and by extension its replication-dependent function, is required to suppress changes in chromatin structure, we expressed the helicase-dead variant of FANCJ in wild-type cells. We reasoned that if the helicase activity prevents chromatin compaction then expression of the dominant-negative mutant should lead to a progressive change in chromatin accessibility. To test this, we generated four independent clones of WT DT40 stably expressing the helicase-dead FANCJ-K52R dominant-negative version of the protein. Importantly, this mutant is defective in promoting processive DNA synthesis and displays an increased level of stalled forks (Fig. 2, C and D; and Fig. 3 C). After expanding the individual clones for three weeks (45 doubling times), we found that chromatin in these clones was more resistant to nuclease cleavage than in WT cells (Fig. 7, A and B; and Fig. S5, A and B). Considering that catalytically inactive FANCJ protein impairs timely progression through S phase, presumably by inhibiting efficient processing of structural DNA barriers (Kumaraswamy and Shiekhattar, 2007), our data suggest that an inability to maintain processive DNA synthesis could drive the reorganization of chromatin structure in this genetic background. However, we could not formally exclude two other possibilities: (1) FANCJ suppresses heterochromatin formation and thereby facilitates the progression of replication forks (Wolffe, 1997), or (2) there is no functional interaction between facilitating fork progression by FANCJ and suppression of chromatin structure reorganization. Therefore, in order to strengthen our initial hypothesis we analyzed the effect of impeding replication by using a low dose of HU or telomestatin on chromatin structure in WT DT40 cells. If correct, our hypothesis would predict that such exposure, inhibiting processive DNA synthesis, should increase chromatin compaction, which is indeed what we observe for both compounds (Fig. 7, C–F; and Fig. S5 C). Furthermore, FANCJ's role in this process seems to be FA core complex independent as ΔFANCC cells show a wild-type digestion pattern (Fig. S5 D). Taken together, our data show

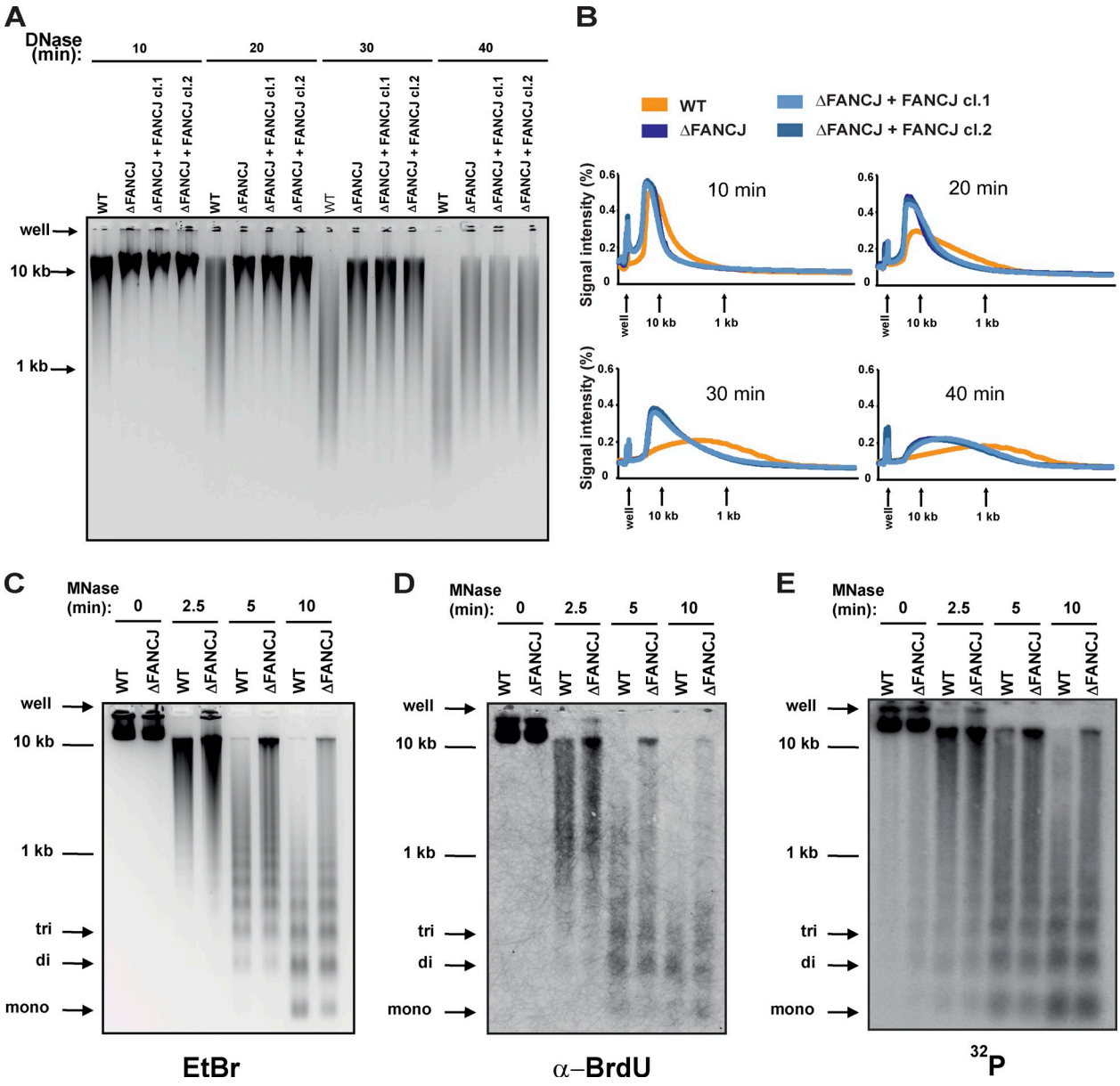

Figure 6. **Changes to chromatin structure in ΔFANCJ cells are irreversible and result from defective maturation of newly replicated daughter strands.** (A) DNase I digest of nuclei from ΔFANCJ cells complemented with WT FANCJ cDNA and (B) signal intensity quantification of A. (C) MNase-digested DNA from WT and ΔFANCJ nuclei was separated on an agarose gel and stained with ethidium bromide. (D) Before MNase digestion, cells were pulse-labeled with BrdU for 15 min. The gel from C was transferred onto a membrane and probed with an anti-BrdU antibody. (E) The membrane from D was hybridized with MNase-digested, ^{32}P-CTP–labeled WT DNA serving as a transfer efficiency control.

that FANCJ helicase activity is required for efficient DNA synthesis during fork passage over difficult to replicate templates, and inability to do so leads to increased condensation of the genome and the subsequent reorganization of chromatin structure.

Unscheduled histone H3 incorporation contributes to reorganization of chromatin structure in FANCJ mutants

Failure to maintain continuous DNA synthesis in the presence of HU has recently been shown to influence the interaction between ASF1, a histone chaperone that buffers excess histones under stressful conditions, and the replisome component MCM2-7 helicase complex. This inherently transient interaction becomes more stable upon fork stalling, leading to an increased accumulation of the newly synthesized histone H3 within the inactive replisome, including histone H3 carrying the predeposition mark K9me1 (Jasencakova et al., 2010). Given that H3K9me1 can be converted into H3K9me3 by Suv39h, an unscheduled fork restart could drive a preferential incorporation of this mark along the newly synthesized DNA contributing to the dynamic reorganization of chromatin structure (Maison et al., 2010). To assess the influence of fork stalling on histone H3 dynamics in ΔFANCJ cells we analyzed the level of H3 trapped with ASF1 in this mutant. To this end, we generated WT and ΔFANCJ cells expressing human strep tagged ASF1a protein (avian cells have only one ASF1 homologue—ASF1a,

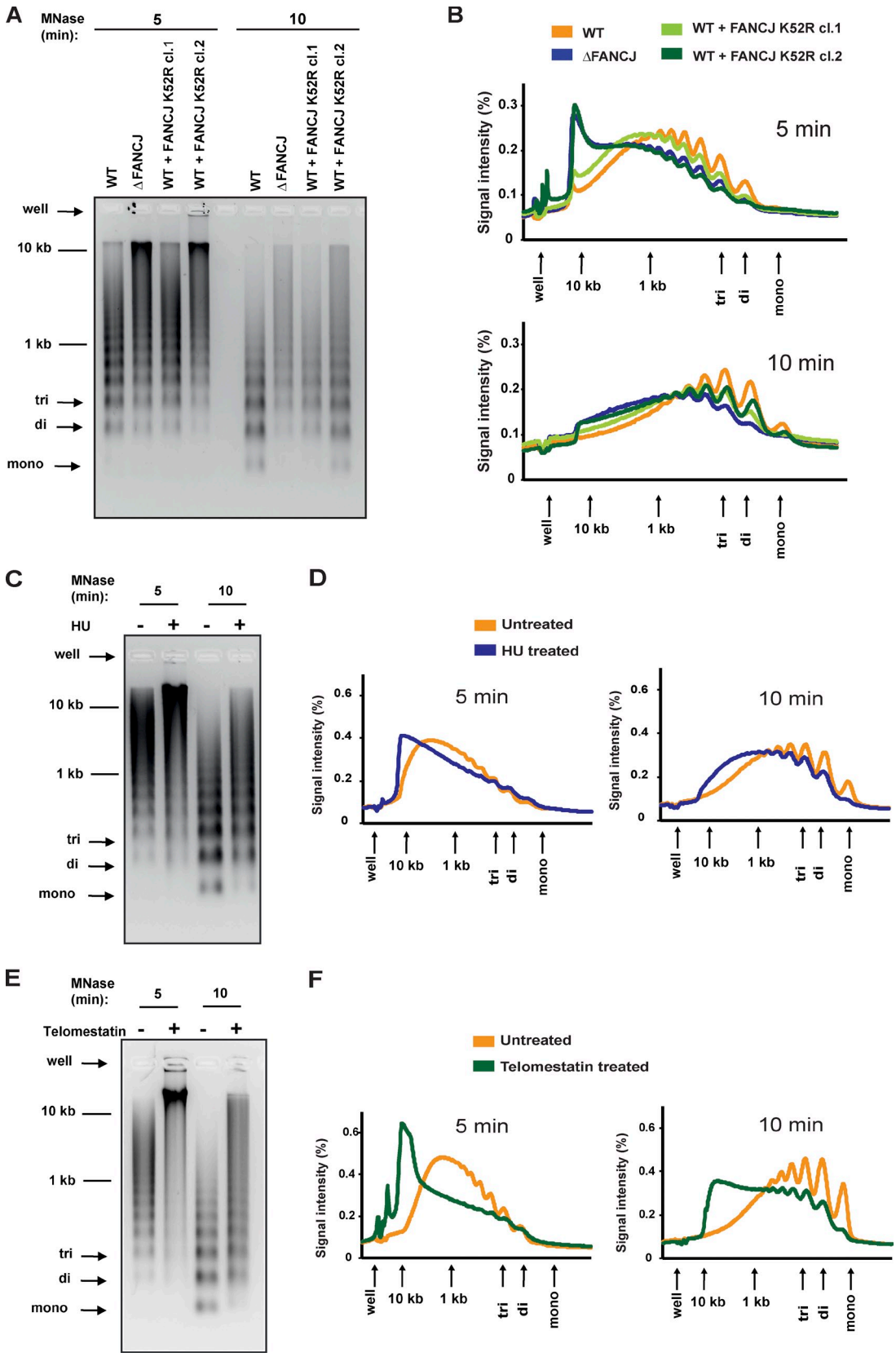

Figure 7. **Impediment to replication fork processivity impacts on chromatin structure.** (A) Nuclei from WT cells complemented with FANCJ K52R cDNA were digested with MNase for times indicated and (B) signal intensity quantification of A. (C) MNase I digest of nuclei from WT DT40 cells grown in the presence of HU (0.2 mM for 7 d followed by 7 d recovery), and (D) signal intensity quantification of C, or (E) telomestatin (5 μM for 7 d followed by 7 d recovery), and (F) signal intensity quantification of E.

which is 100% identical at the amino acid level with its human counterpart; Sanematsu et al., 2006) and then performed a large-scale ASF1 immunoprecipitation from untreated cells, and cells incubated with a dose of HU that does not induce fork stalling (as measured by an increase in fork asymmetry) in WT cells but does so in FANCJ mutant cells. In line with the notion that fork stalling stabilizes the ASF1–MCM2-7 interaction (Jasencakova et al., 2010), we also noticed an increased association of strep-tagged ASF1 with MCM2 protein in ΔFANCJ cells but not in the WT control (Fig. 8 A), which also supports our fiber data (Fig. 3 B). We also noticed an increase in the total amount of ASF1-associated histone H3 in ΔFANCJ cells, and this increase was also reflected in the elevated level of H3 carrying the pre-deposition mark K9me1 (Fig. 8, A and B). Moreover, the ratio of H3 to H3K9me1 in WT and FANCJ mutants was 1:1.3 and 1:1.6 in untreated and treated cells, respectively (Fig. 8 C). Considering that in ΔFANCJ cells stalled forks remain replication proficient we hypothesized that ASF1-bound histones, including H3K9me1, could become rapidly incorporated onto the newly synthesized DNA upon fork restart due to, for example, a repriming event downstream from the blockade. Because conversion of H3K9me1 to H3K9me3 has been implicated in heterochromatin assembly (Loyola and Almouzni, 2007; Maison et al., 2010), we propose that its unscheduled incorporation in FANCJ-deficient cells could drive the reorganization of chromatin structure.

Discussion

Strict maintenance of replication fork integrity is vitally important for dividing cells in the face of genotoxic stress and/or natural replication fork barriers, which can lead to replisome stalling and/or collapsing. This not only ensures accurate DNA replication but also prevents genomic instability, a recognized causative factor in tumor development. In this study, we report that the breast tumor suppressor and Fanconi anemia–related helicase FANCJ supports global replication fork dynamics by promoting processive DNA synthesis under conditions of replicative stress. This is based on the following findings: first, in the absence of FANCJ, replication fork velocity is significantly decreased under low doses of HU or the highly specific G4 quadruplex–stabilizing ligand telomestatin; second, analysis of asymmetry of bidirectional (sister) forks revealed that reduced DNA synthesis is not due to an impaired polymerization step but is rather a consequence of increased fork stalling in the FANCJ-null background. Surprisingly, and unlike the other FA-associated helicase FANCM, FANCJ does not seem to be required to stabilize stalled replication forks, as we were unable to detect any increase in fork collapse in this mutant compared with the control. Moreover, stalled forks remained replication competent and capable of restarting DNA synthesis upon removal of replicative stress, albeit with slightly delayed kinetics. In our opinion this most likely reflects the time needed for the replication machinery to remove the blockade. Our data, however, do not preclude the possibility that in the absence of FANCJ a small proportion of stalled forks may collapse during replication of repetitive runs of G-rich sequences, in line with their increased probability to form G4 quartets (Maizels, 2006). Indeed, clusters of G4 sequence motifs were found near the breakpoints of some deleted regions in FA-J patient and DT40 FANCJ mutant cells (London et al., 2008; Kitao et al., 2011).

It has recently been proposed that FANCJ may support resolution of G-quadruplexes during leading-strand replication (Sarkies et al., 2012). Our data, however, suggest that FANCJ most likely participates in promoting processive DNA synthesis past structured DNA on the lagging strand. This is based on the fact that ΔFANCJ cells accumulate small ssDNA gaps, possibly resulting from repriming events on the lagging strand that correspond in size to the gaps generated in the absence of Polδ, a polymerase required for primer extension during lagging-strand DNA synthesis (Fukui et al., 2004). Such unscheduled repriming could also explain the relatively efficient fork restart seen in this mutant, preventing prolonged fork stalling that could result in replication fork collapse (Petermann et al., 2010). Given that inter-fork distances in DT40 cells are around 37 kb on average (Maya-Mendoza et al., 2007), high molecular DNA fragments (>10 kb) would be predicted to arise from T4 polymerase–dependent extension of a blocked leading-strand DNA synthesis (Fukui et al., 2004). However, we were unable to detect any excess of such events in ΔFANCJ over the WT background. Considering that the footprint of the CMG replication complex (Cdc45, MCM2-7, and GINS) arrested on a leading-strand blockade is around 70 bp (Fu et al., 2011), it is unlikely that the leading-strand polymerase, which is located behind the CMG complex, would be blocked adjacent to the G4 structure impeding the subsequent leading-strand primer extension in the gap-filling assay. Moreover, we can clearly see the formation of such high molecular weight fragments in FANCJ mutant cells treated with MMS, an agent that equally affects leading- and lagging-strand synthesis (unpublished data). It is conceivable that the blocked fork could be rescued by a replisome arriving from an adjacent origin. However, this seems unlikely given that we did not observe a significant increase in interspersed forks (closely spaced initiation and termination events) or origin firing during the HU treatment and fork restart experiments described above. Another possibility is that stalling of the leading strand (i.e., formation of G4 structures) is a rare event that precludes its detection due to the limitation in sensitivity of the assay, or alternatively that FANCJ does not play a major role in promoting leading-strand synthesis past the G4 structures. In support of the latter, polarities of the deletions found in *dog-1* mutants (FANCJ homologue in *C. elegans*) as well as in human FANCJ-deficient cells also suggest that FANCJ unwinds G4 DNA structures forming on the lagging strand during DNA replication (Cheung et al., 2002; Kruisselbrink et al., 2008; London et al., 2008).

Unaltered fork integrity in our mutant poses a question: why are these cells sensitive to a broad spectrum of replication inhibitors? One plausible explanation is that interfering with replication fork movement exacerbates the requirements for a near-perfect template for replication. Thus, FANCJ could function to clear up natural, DNA sequence–dependent replication fork barriers ahead of the advancing replisome. This hypothesis is supported by the fact that the presence of telomestatin, a potent and specific G4 stabilizer, impairs fork movement in

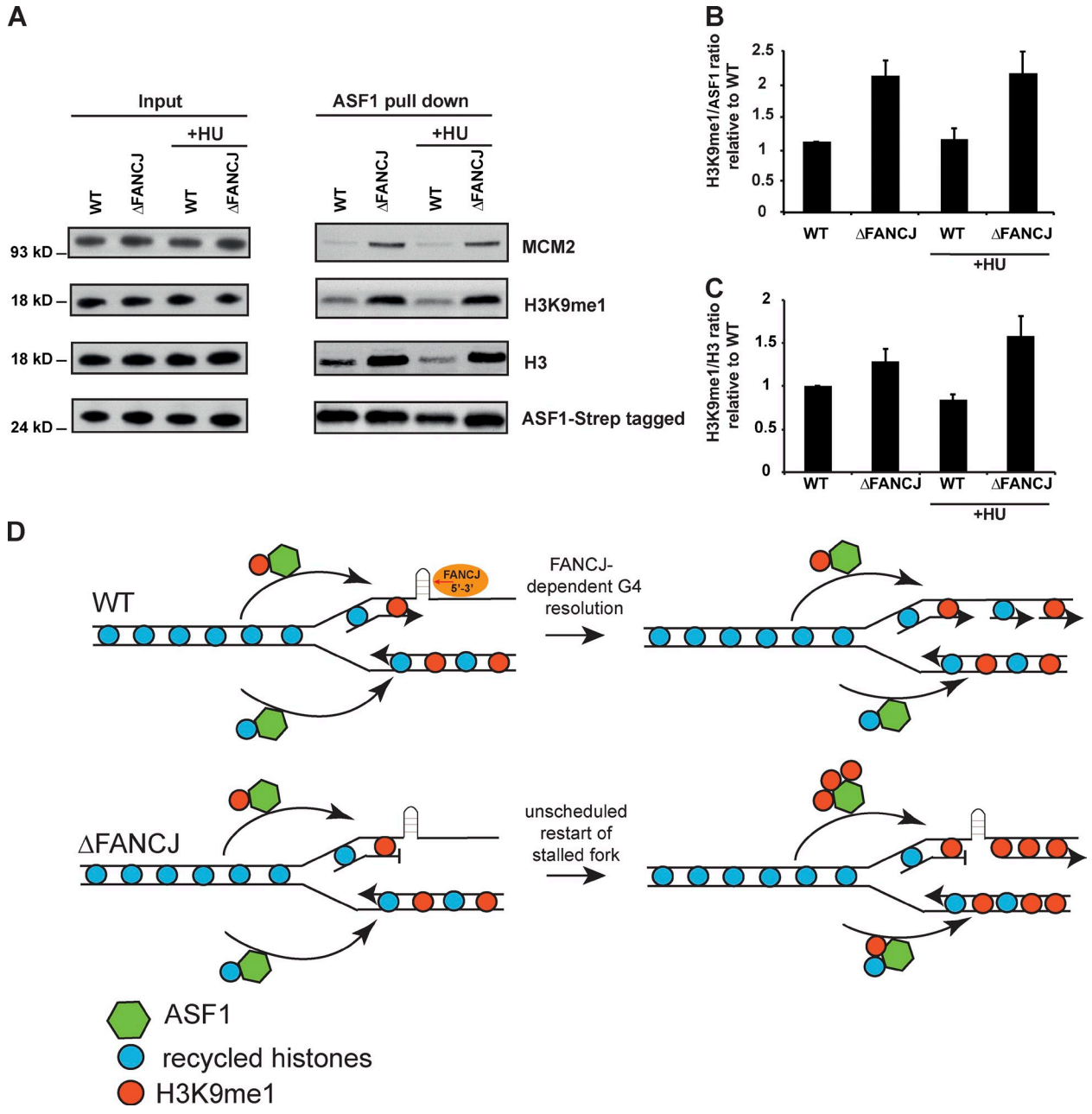

Figure 8. **FANCJ couples fork movement with maintenance of chromatin structure.** (A) Western blot analysis of ASF1 complexes from WT and ΔFANCJ cells. (B and C) Charts showing H3K9me1/ASF1 and H3K9me1/H3 quantified signal ratio relative to untreated WT; ratio set as 1 ($n \geq 3$). (D) Model of FANCJ-dependent coupling of fork movement with maintenance of chromatin architecture. Top: FANCJ resolves G4 structures on the lagging strand allowing for processive DNA synthesis past DNA structure–dependent blockades. Bottom: in the absence of FANCJ a replication fork stalls at the G4 structure, which leads to accumulation of H3K9me1. Upon fork restart unscheduled incorporation of the newly synthesized histones, including H3K9me1, promotes reorganization of chromatin structure.

ΔFANCJ cells but not in the wild-type control. Cells challenged with replication inhibitors accumulate ssDNA and the formation of G4 quadruplexes could be energetically favorable in ssDNA. Therefore, replicative stress could specifically enforce requirements for proteins/pathways dealing with DNA secondary structures. In line with this, *Saccharomyces cerevisiae* Pif1-deficient cells display increased sensitivity to the presence of G4 motifs when cells are challenged with HU. Importantly, this phenotype could be reversed by the removal of DNA sequences able to form G4 quadruplex motifs (Paeschke et al., 2011). Therefore, it seems likely that the sensitivity of FANCJ-deficient cells to replication inhibitors results from destabilizing replisome movement under conditions where the priming and elongation step of DNA synthesis is limited.

Impediments to fork movement could pose a double threat to cell viability, first by challenging the integrity of the DNA and second by interfering with chromatin maturation. In support of this we revealed a significant association between deregulated replication and maturation of chromatin in FANCJ-deficient cells. We showed that an increased association of

ASF1 with the replisome component MCM2 in ΔFANCJ cells correlates with an increased accumulation of the newly synthesized histone H3, including its heterochromatin formation–priming H3K9me1 form, in the vicinity of stalled forks. These findings led us to propose a model (Fig. 8 C) in which we postulate that replisomes blocked in the absence of FANCJ stall, but remain in a replication-competent configuration. This allows the efficient restart of DNA synthesis once the impediment is removed, either by the engagement of an alternative pathway or a repriming event downstream of the blockade. The latter, however, could result in an unreplicated ssDNA gap left behind the fork. We hypothesize that upon removal of the impediments by an alternative pathway and/or a repriming event downstream of the lesion fork restart would create a high demand for ASF1-associated histones, including the H3K9me1 that could contribute to chromatin compaction. In line with this, it has recently been shown that interference with lagging-strand polymerase influences the assembly of newly replicated daughter genomes in *S. cerevisiae* (Smith and Whitehouse, 2012). Alternative but not mutually exclusive possibilities include a delay in the resolution of structured DNA in FANCJ mutants resulting in restarting stalled forks later in S phase, thus promoting heterochromatin assembly via a mechanism proposed by Cedar and colleagues (Lande-Diner et al., 2009) whereby a shift in replication timing affects histone acetylation during nucleosome assembly, leading to heterochromatin formation. We also cannot rule out the possibility that FANCJ somehow facilitates access of nucleosome-remodeling factors to at least a subset of forks paused on natural replication barriers. Indeed, depletion of chromatin-remodeling factors promotes heterochromatin formation on a global scale (Poot et al., 2004). On the other hand, de novo incorporation of newly synthesized histones after post-replicative repair of ssDNA gaps in the FANCJ mutant could counteract heterochromatization and/or even, in some instances (large gaps), could promote local euchromatin expansion (Groth et al., 2007). One potential consequence of chromatin structure reorganization could be a large-scale alteration in the overall transcriptional activity. Accordingly, recent transcriptional profiling of FANCJ-deficient cells detected changes in the gene expression pattern for a subset of genes that are enriched for G4 quadruplex–forming motifs (Sarkies et al., 2012). The data presented here suggest that at least gene silencing in ΔFANCJ mutants could be associated with accumulation of H3K9me3 facilitating changes in chromatin compaction. However, the mechanism that drives up-regulation of gene expression remains unclear. It is tempting to speculate that this could be influenced by position of the transcribed (coding) strand with respect to an origin of replication (leading/lagging) as well as the number and/or position of G-quadruplex–forming motifs within the gene locus. The latter could determine the choice of the repair pathway used to resolve the lesion (i.e., post-replicative repair versus fork restart). Interestingly, G-quadruplex–forming DNA motifs have recently been shown to be enriched within DNA signatures of replication origins in human cells (Besnard et al., 2012). This is important, as guanine-rich sequences are also found in the promoter regions of many tumor suppressor genes and changes in chromatin compaction may result in their silencing (Eddy and Maizels, 2006). Heterochromatin has also been reported to restrain the DNA damage response (Goodarzi et al., 2010). Given that the computational analysis of the human and avian genomes reveals the existence of more than 360,000 potential G4 motifs (Huppert and Balasubramanian, 2005; unpublished data), it is reasonable to assume that heterochromatization seen in FANCJ mutant cells could have an important role in restraining activation of DNA damage response signaling pathways in order to promote replication under constitutive replicative stress.

In summary, our data firmly establish a role for FANCJ in facilitating replication fork progression with maintenance of chromatin structure. Because both genomic and epigenetic instability have been linked to tumorigenesis (Podlaha et al., 2012), our data also underscore the importance of controlling replication fork movements on the level of replisome stability as well as replication rate. Finally, given that DNA sequences with the ability to form G4 quadruplex structures are highly abundant throughout the human genome, we speculate that targeting proteins that bind and/or process such structures has the potential to interfere with cell survival. Therefore, inhibitors of FANCJ's enzymatic activity could be exploited therapeutically to boost the toxicity of compounds interfering with replication.

Materials and methods

Cells and plasmids

Chicken DT40 cells were cultured at 38°C in RPMI 1640 medium supplemented with 8% FBS, 2% chicken serum, and 50 µM β-mercaptoethanol essentially as described previously (Schwab et al., 2010). ΔFANCJ cells were a generous gift from K. Hiom (University of Dundee, Dundee, Scotland, UK; Bridge et al., 2005) and K.J. Patel (MRC LMB, Cambridge, UK; Sarkies et al., 2012). Human wild-type and K52R FANCJ in pOZ (Cantor et al., 2001) and ASF1a in pEXPR-IBA105 (Jasencakova et al., 2010) were kindly provided by S. Cantor (University of Massachusetts Medical School, Worcester, MA) and A. Groth (BRIC, University of Copenhagen, Copenhagen, Denmark), respectively. FANCJ cDNA was excised with NotI–XhoI and inserted into pcDNA3.1(−); constructs were randomly integrated by electroporation.

Cell survival assays

MTS survival assays were performed as described previously (Schwab et al., 2010). In brief, 3×10^3 cells/well in 96-well plates were untreated or treated with indicated doses of camptothecin, hydroxyurea, and aphidicolin (all from Sigma-Aldrich) and incubated for five cell doubling times. MTS reagent (Promega) was added to each well and absorbance was measured at 492 nm after 4 h incubation at 37°C.

DNA fiber analysis

DNA fiber analyses were performed as described previously (Schwab et al., 2010; Schwab and Niedzwiedz, 2011). In brief, exponentially growing DT40 cells were first incubated with 25 µM iododeoxyuridine (IdU) and then with 250 µM chlorodeoxyuridine (CldU) for the indicated times. Fiber spreads were prepared from 10^6 cells/ml. Slides were incubated in 2.5 M HCl for 80 min, washed in PBS, and then incubated in blocking buffer (2% BSA in PBS) for 20 min. Next, slides were incubated for 1 h with primary antibodies diluted in blocking buffer, washed several times in PBS, and then incubated with secondary antibodies for 30 min. Slides were removed and mounted using Vectashield mounting medium (Vector Laboratories). A confocal microscope (LSM 510 Meta; Carl Zeiss) equipped with Plan-Apochromat 63×/1.4 oil DIC objective was used to collect fiber images from randomly selected fields at RT using LSM software (Carl Zeiss). Analysis was performed using the ImageJ software package (National Institutes of Health). Replication elongation assays were performed by labeling cells with IdU for 20 min followed by treatment with CldU in combination with 0.2 mM HU for 40 min, unless stated otherwise. A minimum of 100 fibers per experiment from at least three independent experiments was scored. Student's two-tailed *t* test was used

to determine statistical significance. Sister forks were selected and measured from pictures from three independent experiments. At least 50 tract-length ratios were plotted.

Gap assay

1.5 µg of genomic DNA was incubated with 7.5 units of T4 DNA polymerase (Thermo Fisher Scientific), dNTPs, and α-[^{32}P]ATP at 37°C in a buffer containing 67 mM Tris-HCl, pH 8.8, 6.6 mM $MgCl_2$, 1 mM DTT, and 16.8 mM $(NH_4)_2SO_4$. DNA was separated on a denaturing 1% agarose gel before transfer.

Western blotting

Western blotting was performed as described previously (Schwab et al., 2010) with the following antibodies: FANCJ (Sigma-Aldrich); H3, MCM2, H3K4me3, and H3K9me3 (Abcam); H3K9me1 (EMD Millipore); H3K9Ac and H3K27Ac (Active Motif); Strep tag (PromoKine); and BrdU (BD). Blots were quantified with ImageQuant 5.2 software (GE Healthcare) or Odyssey infrared Western blotting system (histone modifications; LI-COR Biosciences). Data represent mean ± SEM from at least three independent experiments.

Acid cell extract preparation

10^7 cells were washed twice with PBS, resuspended in 0.1 ml 0.2 M HCl, and incubated on ice for 1 h. After centrifugation, histone-containing supernatant was harvested and neutralized with 1 M Tris-HCl, pH 8.0.

MNase and DNase I digest

2×10^7 cells were washed twice with PBS, resuspended in hypotonic buffer (10 mM Tris-HCl, pH 7.5, 2 mM $MgCl_2$, 3 mM $CaCl_2$, 320 mM sucrose, and 1 mM DTT), and incubated on ice for 10 min. IGEPAL-CA630 was added to a final concentration of 0.3% and samples were briefly vortexed before centrifugation. Nuclei were washed and resuspended in MNase digestion buffer (10 mM Tris-HCl, pH 7.5, 15 mM NaCl, 60 mM KCl, 1 mM $CaCl_2$, and 250 mM sucrose; for DNase I digestion supplemented with 2 mM $MgCl_2$). MNase digestion (2.5 U/50 µl) was performed at 25°C and DNase I (5 U/50 µl) at 37°C. Reaction was stopped with 20 mM EDTA and 2 mM EGTA. Genomic DNA was extracted by proteinase K digestion, phenol/chloroform extraction, and RNase A digestion. 2.5 µg DNA was separated on a gel. Signal intensity was quantified with ImageQuant TL and presented as a percentage of the total (for each lane) across the distance from the well to the end of the gel.

Southern blotting

Southern blot probes were amplified with following primers: β-globin locus, 5′-GTAAATCCTCCCTTGGGACTCCATAC-3′ and 5′-TTCTTCCCTCTGGAGCAATCAGAC-3′; $V\lambda_R$, 5′-GCCGTCACTGATTGCCGTTTTCTCCCCTC-3′ and 5′-CGAGACGAGGTCAGCGACTCACCTAGGAC-3′; CD72, 5′-CACCACGTTGCTACCATGCTGTC-3′ and 5′-AGGGCAGGAGAGCAGGAAAGAAG-3′; Bu1a, 5′-CTCTGTAGCCAGATCGTCTTCTC-3′ and 5′-CCTGCACTCAAATCCCAGATG-3′.

EpiQ chromatin analysis

Q-PCR–based EpiQ chromatin analysis assay (Bio-Rad Laboratories) was performed according to the manufacturer's protocol. PCR primers were as follows: constitutively condensed β-globin locus, 5′-GGAACAAGTTGGCAAGGTCCTAT-3′ and 5′-TCTTCTGCCCTGCCCGTAT-3′ (Litt et al., 2001); ovalbumin, 5′-AACTTCTCACCTGTGTATGCATTC-3′ and 5′-ATCAGGCAAACTGCAAAGCATATC-3′; $V\lambda_R$, 5′-GCCGTCACTGATTGCCGTTTTCTCCCCTC-3′ and 5′-CGAGACGAGGTCAGCGACTCACCTAGGAC-3′ (Cummings et al., 2007); CD72, 5′-CAAGTTCTGCTTCTGTAAGAGCC-3′ and 5′-AGGTCAGTGTAGAGCACTCCTTG-3′; Bu1a, 5′-CTCTGTAGCCAGATCGTCTTCTC-3′ and 5′-GTGTCAGCTCATCTAGGCAAATC-3′ (Sarkies et al., 2012). Data represent at least four independent experiments. Student's two-tailed *t* test was used to determine statistical significance.

Comet assay

Cells were untreated or treated with 10 mM HU for 6 h and comet assay was performed as described in Wojewódzka et al. (2002). In brief, cells were resuspended in PBS (10^5 cells/ml) and mixed with an equal volume of 1.5% agarose type VII in PBS at 37°C. The suspension was cast on a microscope slide precoated with 0.5% agarose type IA. Cells were lysed for 1 h at 4°C in lysis buffer (2.5 M NaCl, 0.1 M EDTA, 10 mM Tris, 1% sarcosyl, 10% DMSO, and 0.5% Triton X-100, pH 9.5). Electrophoresis was performed in buffer containing 300 mM sodium acetate, 100 mM Tris, pH 8.5, at 0.8 V/cm for 1 h at 4°C. Comets were stained with SybrGold and analyzed with Komet 6 (Andor Technology). 30 comets per experiment from at least three independent experiments were scored.

ASF1 complex purification

Cells were washed with PBS before lysis in buffer containing 50 mM Tris-HCl, pH 7.5, 150 mM NaCl, 1 mM $MgCl_2$, 5 mM NaF, 0.5% Igepal CA-630, 25 U/ml benzonase, and protease inhibitors. Cleared lysates were adjusted to achieve final buffer concentration of 50 mM Tris-HCl, pH 7.5, 150 mM NaCl, 0.5 mM $MgCl_2$, 1 mM EDTA, 5 mM NaF, and 0.25% Igepal CA-630, and incubated with streptactin resin (IBA) at 4°C for 2 h. ASF1-associated complexes were eluted by boiling beads in Laemmli buffer.

Online supplemental material

Fig. S1 shows replication fork dynamics in untreated FANCJ-deficient cells. Fig. S2 shows elongation fork rates in WT and ΔFANCJ cells treated with 1 mM of HU for 20 and 40 min. Fig. S3 shows changes in chromatin state within euchromatic and heterochromatic regions analyzed by Southern blot, and the level of chromatin accessibility in two independently derived ΔFANCJ clones. Fig. S4 shows defective maturation of newly replicated chromatin in ΔFANCJ cells analyzed by DNase I digest. Fig. S5 shows chromatin accessibility to MNase digest in WT cells expressing FANCJ-K52R mutant protein and quantification of histone marks in WT DT40 cells exposed for a prolonged time to HU or telomestatin. Online supplemental material is available at http://www.jcb.org/cgi/content/full/jcb.201208009/DC1.

We would like to thank K. Hiom, K.J. Patel, S. Cantor and A. Groth for reagents; M. Kruszewski and M. Wojewodzka for technical assistance with the comet assay; and P. McHugh and A. Blackford for critical reading of the manuscript. Finally, we would like to thank the reviewers for their helpful comments.

This work was supported by the Senior International Research Fellowship from the Association for International Cancer Research and MRC Senior Research Fellowship (to W. Niedzwiedz) and the Polish Ministry of Science and Higher Education Fellowship (to J. Nieminuszczy).

The authors declare no conflicts of interest.

Submitted: 6 August 2012
Accepted: 26 February 2013

References

Bell, O., V.K. Tiwari, N.H. Thomä, and D. Schübeler. 2011. Determinants and dynamics of genome accessibility. *Nat. Rev. Genet.* 12:554–564. http://dx.doi.org/10.1038/nrg3017

Besnard, E., A. Babled, L. Lapasset, O. Milhavet, H. Parrinello, C. Dantec, J.M. Marin, and J.M. Lemaitre. 2012. Unraveling cell type-specific and reprogrammable human replication origin signatures associated with G-quadruplex consensus motifs. *Nat. Struct. Mol. Biol.* 19:837–844. http://dx.doi.org/10.1038/nsmb.2339

Blackford, A.N., R.A. Schwab, J. Nieminuszczy, A.J. Deans, S.C. West, and W. Niedzwiedz. 2012. The DNA translocase activity of FANCM protects stalled replication forks. *Hum. Mol. Genet.* 21:2005–2016. http://dx.doi.org/10.1093/hmg/dds013

Branzei, D., and M. Foiani. 2010. Maintaining genome stability at the replication fork. *Nat. Rev. Mol. Cell Biol.* 11:208–219. http://dx.doi.org/10.1038/nrm2852

Bridge, W.L., C.J. Vandenberg, R.J. Franklin, and K. Hiom. 2005. The BRIP1 helicase functions independently of BRCA1 in the Fanconi anemia pathway for DNA crosslink repair. *Nat. Genet.* 37:953–957. http://dx.doi.org/10.1038/ng1627

Cantor, S.B., D.W. Bell, S. Ganesan, E.M. Kass, R. Drapkin, S. Grossman, D.C. Wahrer, D.C. Sgroi, W.S. Lane, D.A. Haber, and D.M. Livingston. 2001. BACH1, a novel helicase-like protein, interacts directly with BRCA1 and contributes to its DNA repair function. *Cell.* 105:149–160. http://dx.doi.org/10.1016/S0092-8674(01)00304-X

Cheung, I., M. Schertzer, A. Rose, and P.M. Lansdorp. 2002. Disruption of dog-1 in *Caenorhabditis elegans* triggers deletions upstream of guanine-rich DNA. *Nat. Genet.* 31:405–409.

Conti, C., B. Saccà, J. Herrick, C. Lalou, Y. Pommier, and A. Bensimon. 2007. Replication fork velocities at adjacent replication origins are coordinately modified during DNA replication in human cells. *Mol. Biol. Cell.* 18:3059–3067. http://dx.doi.org/10.1091/mbc.E06-08-0689

Cummings, W.J., M. Yabuki, E.C. Ordinario, D.W. Bednarski, S. Quay, and N. Maizels. 2007. Chromatin structure regulates gene conversion. *PLoS Biol.* 5:e246. http://dx.doi.org/10.1371/journal.pbio.0050246

Eddy, J., and N. Maizels. 2006. Gene function correlates with potential for G4 DNA formation in the human genome. *Nucleic Acids Res.* 34:3887–3896. http://dx.doi.org/10.1093/nar/gkl529

Fu, Y.V., H. Yardimci, D.T. Long, T.V. Ho, A. Guainazzi, V.P. Bermudez, J. Hurwitz, A. van Oijen, O.D. Schärer, and J.C. Walter. 2011. Selective bypass of a lagging strand roadblock by the eukaryotic replicative DNA helicase. *Cell*. 146:931–941. http://dx.doi.org/10.1016/j.cell.2011.07.045

Fukui, T., K. Yamauchi, T. Muroya, M. Akiyama, H. Maki, A. Sugino, and S. Waga. 2004. Distinct roles of DNA polymerases delta and epsilon at the replication fork in Xenopus egg extracts. *Genes Cells*. 9:179–191. http://dx.doi.org/10.1111/j.1356-9597.2004.00716.x

Goodarzi, A.A., P. Jeggo, and M. Lobrich. 2010. The influence of heterochromatin on DNA double strand break repair: Getting the strong, silent type to relax. *DNA Repair (Amst.)*. 9:1273–1282. http://dx.doi.org/10.1016/j.dnarep.2010.09.013

Groth, A., W. Rocha, A. Verreault, and G. Almouzni. 2007. Chromatin challenges during DNA replication and repair. *Cell*. 128:721–733. http://dx.doi.org/10.1016/j.cell.2007.01.030

Gupta, R., S. Sharma, J.A. Sommers, Z. Jin, S.B. Cantor, and R.M. Brosh Jr. 2005. Analysis of the DNA substrate specificity of the human BACH1 helicase associated with breast cancer. *J. Biol. Chem.* 280:25450–25460. http://dx.doi.org/10.1074/jbc.M501995200

Hiom, K. 2010. FANCJ: solving problems in DNA replication. *DNA Repair (Amst.)*. 9:250–256. http://dx.doi.org/10.1016/j.dnarep.2010.01.005

Huppert, J.L., and S. Balasubramanian. 2005. Prevalence of quadruplexes in the human genome. *Nucleic Acids Res.* 33:2908–2916. http://dx.doi.org/10.1093/nar/gki609

Jasencakova, Z., A.N. Scharf, K. Ask, A. Corpet, A. Imhof, G. Almouzni, and A. Groth. 2010. Replication stress interferes with histone recycling and predeposition marking of new histones. *Mol. Cell*. 37:736–743. http://dx.doi.org/10.1016/j.molcel.2010.01.033

Kitao, H., I. Nanda, R.P. Sugino, A. Kinomura, M. Yamazoe, H. Arakawa, M. Schmid, H. Innan, K. Hiom, and M. Takata. 2011. FancJ/Brip1 helicase protects against genomic losses and gains in vertebrate cells. *Genes Cells*. 16:714–727. http://dx.doi.org/10.1111/j.1365-2443.2011.01523.x

Kruisselbrink, E., V. Guryev, K. Brouwer, D.B. Pontier, E. Cuppen, and M. Tijsterman. 2008. Mutagenic capacity of endogenous G4 DNA underlies genome instability in FANCJ-defective *C. elegans*. *Curr. Biol.* 18:900–905. http://dx.doi.org/10.1016/j.cub.2008.05.013

Kumaraswamy, E., and R. Shiekhattar. 2007. Activation of BRCA1/BRCA2-associated helicase BACH1 is required for timely progression through S phase. *Mol. Cell. Biol.* 27:6733–6741. http://dx.doi.org/10.1128/MCB.00961-07

Lande-Diner, L., J. Zhang, and H. Cedar. 2009. Shifts in replication timing actively affect histone acetylation during nucleosome reassembly. *Mol. Cell*. 34:767–774. http://dx.doi.org/10.1016/j.molcel.2009.05.027

Lemarteleur, T., D. Gomez, R. Paterski, E. Mandine, P. Mailliet, and J.F. Riou. 2004. Stabilization of the c-myc gene promoter quadruplex by specific ligands' inhibitors of telomerase. *Biochem. Biophys. Res. Commun.* 323:802–808. http://dx.doi.org/10.1016/j.bbrc.2004.08.150

Litman, R., M. Peng, Z. Jin, F. Zhang, J. Zhang, S. Powell, P.R. Andreassen, and S.B. Cantor. 2005. BACH1 is critical for homologous recombination and appears to be the Fanconi anemia gene product FANCJ. *Cancer Cell*. 8:255–265. http://dx.doi.org/10.1016/j.ccr.2005.08.004

Litt, M.D., M. Simpson, F. Recillas-Targa, M.N. Prioleau, and G. Felsenfeld. 2001. Transitions in histone acetylation reveal boundaries of three separately regulated neighboring loci. *EMBO J.* 20:2224–2235. http://dx.doi.org/10.1093/emboj/20.9.2224

London, T.B., L.J. Barber, G. Mosedale, G.P. Kelly, S. Balasubramanian, I.D. Hickson, S.J. Boulton, and K. Hiom. 2008. FANCJ is a structure-specific DNA helicase associated with the maintenance of genomic G/C tracts. *J. Biol. Chem.* 283:36132–36139. http://dx.doi.org/10.1074/jbc.M808152200

Loyola, A., and G. Almouzni. 2007. Marking histone H3 variants: how, when and why? *Trends Biochem. Sci.* 32:425–433. http://dx.doi.org/10.1016/j.tibs.2007.08.004

Maison, C., J.P. Quivy, A.V. Probst, and G. Almouzni. 2010. Heterochromatin at mouse pericentromeres: a model for de novo heterochromatin formation and duplication during replication. *Cold Spring Harb. Symp. Quant. Biol.* 75:155–165. http://dx.doi.org/10.1101/sqb.2010.75.013

Maizels, N. 2006. Dynamic roles for G4 DNA in the biology of eukaryotic cells. *Nat. Struct. Mol. Biol.* 13:1055–1059. http://dx.doi.org/10.1038/nsmb1171

Maya-Mendoza, A., E. Petermann, D.A. Gillespie, K.W. Caldecott, and D.A. Jackson. 2007. Chk1 regulates the density of active replication origins during the vertebrate S phase. *EMBO J.* 26:2719–2731. http://dx.doi.org/10.1038/sj.emboj.7601714

Paeschke, K., J.A. Capra, and V.A. Zakian. 2011. DNA replication through G-quadruplex motifs is promoted by the Saccharomyces cerevisiae Pif1 DNA helicase. *Cell*. 145:678–691. http://dx.doi.org/10.1016/j.cell.2011.04.015

Petermann, E., M.L. Orta, N. Issaeva, N. Schultz, and T. Helleday. 2010. Hydroxyurea-stalled replication forks become progressively inactivated and require two different RAD51-mediated pathways for restart and repair. *Mol. Cell*. 37:492–502. http://dx.doi.org/10.1016/j.molcel.2010.01.021

Podlaha, O., M. Riester, S. De, and F. Michor. 2012. Evolution of the cancer genome. *Trends Genet.* 28:155–163. http://dx.doi.org/10.1016/j.tig.2012.01.003

Poot, R.A., L. Bozhenok, D.L. van den Berg, S. Steffensen, F. Ferreira, M. Grimaldi, N. Gilbert, J. Ferreira, and P.D. Varga-Weisz. 2004. The Williams syndrome transcription factor interacts with PCNA to target chromatin remodelling by ISWI to replication foci. *Nat. Cell Biol.* 6:1236–1244. http://dx.doi.org/10.1038/ncb1196

Sanders, C.M. 2010. Human Pif1 helicase is a G-quadruplex DNA-binding protein with G-quadruplex DNA-unwinding activity. *Biochem. J.* 430:119–128. http://dx.doi.org/10.1042/BJ20100612

Sanematsu, F., Y. Takami, H.K. Barman, T. Fukagawa, T. Ono, K. Shibahara, and T. Nakayama. 2006. Asf1 is required for viability and chromatin assembly during DNA replication in vertebrate cells. *J. Biol. Chem.* 281:13817–13827. http://dx.doi.org/10.1074/jbc.M511590200

Sarkies, P., C. Reams, L.J. Simpson, and J.E. Sale. 2010. Epigenetic instability due to defective replication of structured DNA. *Mol. Cell*. 40:703–713. http://dx.doi.org/10.1016/j.molcel.2010.11.009

Sarkies, P., P. Murat, L.G. Phillips, K.J. Patel, S. Balasubramanian, and J.E. Sale. 2012. FANCJ coordinates two pathways that maintain epigenetic stability at G-quadruplex DNA. *Nucleic Acids Res.* 40:1485–1498. http://dx.doi.org/10.1093/nar/gkr868

Schwab, R.A., and W. Niedzwiedz. 2011. Visualization of DNA replication in the vertebrate model system DT40 using the DNA fiber technique. *J. Vis. Exp.* 27:e3255.

Schwab, R.A., A.N. Blackford, and W. Niedzwiedz. 2010. ATR activation and replication fork restart are defective in FANCM-deficient cells. *EMBO J.* 29:806–818. http://dx.doi.org/10.1038/emboj.2009.385

Seale, R.L. 1975. Assembly of DNA and protein during replication in HeLa cells. *Nature*. 255:247–249. http://dx.doi.org/10.1038/255247a0

Smith, D.J., and I. Whitehouse. 2012. Intrinsic coupling of lagging-strand synthesis to chromatin assembly. *Nature*. 483:434–438. http://dx.doi.org/10.1038/nature10895

Sogo, J.M., M. Lopes, and M. Foiani. 2002. Fork reversal and ssDNA accumulation at stalled replication forks owing to checkpoint defects. *Science*. 297:599–602. http://dx.doi.org/10.1126/science.1074023

Suhasini, A.N., and R.M. Brosh Jr. 2012. Fanconi anemia and Bloom's syndrome crosstalk through FANCJ-BLM helicase interaction. *Trends Genet.* 28:7–13. http://dx.doi.org/10.1016/j.tig.2011.09.003

Suhasini, A.N., N.A. Rawtani, Y. Wu, J.A. Sommers, S. Sharma, G. Mosedale, P.S. North, S.B. Cantor, I.D. Hickson, and R.M. Brosh Jr. 2011. Interaction between the helicases genetically linked to Fanconi anemia group J and Bloom's syndrome. *EMBO J.* 30:692–705. http://dx.doi.org/10.1038/emboj.2010.362

Wojewódzka, M., I. Buraczewska, and M. Kruszewski. 2002. A modified neutral comet assay: elimination of lysis at high temperature and validation of the assay with anti-single-stranded DNA antibody. *Mutat. Res.* 518:9–20. http://dx.doi.org/10.1016/S1383-5718(02)00070-0

Wolffe, A.P. 1997. Histones, nucleosomes and the roles of chromatin structure in transcriptional control. *Biochem. Soc. Trans.* 25:354–358.

Wu, Y., K. Shin-ya, and R.M. Brosh Jr. 2008. FANCJ helicase defective in Fanconia anemia and breast cancer unwinds G-quadruplex DNA to defend genomic stability. *Mol. Cell. Biol.* 28:4116–4128. http://dx.doi.org/10.1128/MCB.02210-07

Youds, J.L., L.J. Barber, J.D. Ward, S.J. Collis, N.J. O'Neil, S.J. Boulton, and A.M. Rose. 2008. DOG-1 is the *Caenorhabditis elegans* BRIP1/FANCJ homologue and functions in interstrand cross-link repair. *Mol. Cell. Biol.* 28:1470–1479. http://dx.doi.org/10.1128/MCB.01641-07

Zhang, F., Q. Fan, K. Ren, A.D. Auerbach, and P.R. Andreassen. 2010. FANCJ/BRIP1 recruitment and regulation of FANCD2 in DNA damage responses. *Chromosoma*. 119:637–649. http://dx.doi.org/10.1007/s00412-010-0285-6